

A HIGH-RESOLUTION CORAL-BASED $\Delta^{14}\text{C}$ RECORD OF SURFACE WATER PROCESSES IN THE WESTERN MEDITERRANEAN SEA

Nadine Tisnérat-Laborde¹ • Paolo Montagna^{1,2,3} • Malcolm McCulloch⁴ • Giuseppe Siani⁵ • Sergio Silenzi^{6,†} • Norbert Frank^{1,7}

ABSTRACT. The first high-resolution time series of pre- and post-bomb radiocarbon measurements is reported for surface waters in the western Mediterranean Sea. The $\Delta^{14}\text{C}$ record was obtained from the aragonite skeleton of *Cladocora caespitosa* using a 50-yr-old corallite collected in the Ligurian Sea in 1998. Laser-ablation ICP measurements of trace elements (Li/Mg and Sr/Ca) show a strong seasonal variability, enabling the chronology of the $\Delta^{14}\text{C}$ record to be determined at annual time-scales. The mean $\Delta^{14}\text{C}$ of pre-bomb surface water is $-56 \pm 3\text{‰}$, corresponding to a reservoir age of 262 ± 29 yr. The post-bomb maximum occurs in 1972 with a $\Delta^{14}\text{C}$ value of 90‰, significantly lower than the peak of 150‰ observed in the North Atlantic. The dilution of the peak-amplitude of $\Delta^{14}\text{C}$ in western Mediterranean surface waters is attributed to mixing of North Atlantic Central Water inflow with relatively depleted underlying Intermediate Mediterranean and Levantine Intermediate waters. Intensification of this mixing is observed in 1963–1964, consistent with the change in atmospheric circulation from a positive to negative NAO phase (1960–1967). The post-peak $\Delta^{14}\text{C}$ variability is relatively limited, reflecting mainly local vertical mixing forced by wind stress.

INTRODUCTION

Radiocarbon time series of the surface oceans provide a unique opportunity to study both air-sea $^{14}\text{CO}_2$ exchanges and ocean circulation (Broecker et al. 1985; Druffel 1987, 1989; Guilderson and Schrag 1998; Guilderson et al. 2000a,b). Continuous marine ^{14}C records have been obtained for the past several decades from only a limited number of biogenic calcifying archives, such as annually banded tropical corals, mollusk shells, and fish otoliths (Druffel and Linick 1978; Druffel 1987; Weidman and Jones 1993; Guilderson and Schrag 1998; Kalish et al. 2001). These records document the surface oceanic uptake of bomb ^{14}C produced by thermonuclear weapons testing in the late 1950s and early 1960s. They have provided a wealth of information on the timing of uptake and the attenuation rate of bomb-derived marine ^{14}C , as well as invaluable constraints on the processes controlling atmosphere and ocean gas exchange. Additionally, marine ^{14}C records have also been useful in constraining models of carbon cycling in the oceans and the role of upwelling and vertical entrainment and replenishment of differently ventilated (^{14}C -aged) water masses (Toggweiler et al. 1989, 1991; Guilderson et al. 2000a; Rodgers et al. 2004; McCulloch et al. 2010). ^{14}C time series have been obtained for different locations in the Pacific (Konoshi et al. 1982; Druffel 1987; Toggweiler et al. 1991; Druffel et al. 2001; Druffel and Griffin 1993, 1999; Guilderson and Schrag 1998; Guilderson et al. 2000, 2009; Fallon and Guilderson 2008), Indian (Cember 1989; Toggweiler et al. 1991), and Atlantic oceans (Nozaki et al. 1978; Druffel 1989, 1996; Weidman and Jones 1993; Campana et al. 1997; Kalish et al. 2001; Sherwood et al. 2008; Tisnérat-Laborde 2010). However, currently, only sparse ^{14}C data are available for the Mediterranean Sea and those are derived from mol-

¹Laboratoire des Sciences du Climat et de l'Environnement, LSCE/IPSL, UMR 8212 UVSQ-CNRS-CEA, Avenue de la Terrasse, F-91198 Gif-sur-Yvette, France.

²Istituto di Scienze Marine, CNR, Bologna, Italy.

³Lamont-Doherty Earth Observatory of Columbia University, Palisades, New York 10964, USA.

⁴UWA Ocean Institute and ARC Centre of Excellence in Coral Reef Studies, School of Earth and Environment, The University of Western Australia, Perth, Australia.

⁵Laboratoire Interactions et Dynamique des Environnements de Surface IDES, UMR 8148 CNRS-Université Paris-Sud 11, Orsay, France.

⁶Istituto Superiore per la Protezione e la Ricerca Ambientale, Rome, Italy.

⁷Institut für Umweltphysik, Universität Heidelberg, INF229, 69120 Heidelberg, Germany.

lusk shells with a limited age range (Siani et al. 2000; Reimer and McCormac 2002). Recent studies have revealed that the shallow-water zooxanthellate Mediterranean coral *Cladocora caespitosa* can serve as a reliable archive for seawater temperature and pH reconstructions (Peirano et al. 2004; Silenzi et al. 2005; Montagna et al. 2007, 2008; Trotter et al. 2011) and thus is a potentially useful archive for ^{14}C studies.

The Mediterranean Sea is a largely enclosed marine basin located at the boundary between the subtropical and mid-latitude zones. Due to its relatively small size and latitudinal position, the Mediterranean is particularly sensitive to natural climate perturbations both in the past as well as in our current era of human-induced global warming (Rixen et al. 2005; Belkin 2009). Large-scale atmospheric circulation linked to specific atmospheric modes, such as the North Atlantic Oscillation (NAO), East Atlantic pattern (EA), and the East Atlantic-West Russia pattern (EAWR), interact with and impact the Mediterranean air-sea heat flux (Josey et al. 2011), freshwater runoff, and the intermediate and deep water formation, which in turn controls the transfer of heat, salt, oxygen, nutrients and carbon between the surface to the deep layers (Papadopoulos et al. 2012). The NAO, a climate fluctuation associated with differences in the sea-level pressure between the Azores and Iceland, drives changes in the strength and position of the westerlies flowing across the Mediterranean (Hurrell et al. 2003), thereby exerting a dominant influence on wintertime air temperature and sea surface temperature (SST) of the Mediterranean Sea (Trigo et al. 2002; Hurrell and Deser 2009). The EA pattern (Barnston and Livezey 1987) plays an important role in modulating the European and Mediterranean climates and has a larger impact on the air-sea heat exchange in the Mediterranean Sea as compared to NAO. As stated above, ^{14}C is powerful tracer of air-sea gas exchange and ocean circulation. Therefore, high-resolution studies of western Mediterranean Sea (WMS) waters ^{14}C may provide insights into the link between atmospheric forcing such as NAO, and the oceanic response in terms of gas exchange, vertical mixing, and lateral advection.

Here, we report the results of ^{14}C concentrations (given as $\Delta^{14}\text{C}$) analyzed at annual resolution in a 50-yr-old specimen of *Cladocora caespitosa*, which represent the first annual $\Delta^{14}\text{C}$ record for the surface western Mediterranean Sea (Ligurian Sea, Figure 1). These new ^{14}C results exhibit a previously undocumented dynamic $\Delta^{14}\text{C}$ range for the western Mediterranean Sea, most likely reflecting spatially variable oscillations of the ocean-atmosphere and further point to changes of the strength of North Atlantic Central Water (NACW) with Levantine Intermediate Water (LIW) exchange that may be linked to NAO fluctuations.

SAMPLING LOCATION AND HYDROGRAPHIC SETTING

For this study, a portion of a large colony of the zooxanthellate coral *Cladocora caespitosa* was collected in 1998 off the coast of Bonassola (44°10'N, 9°36'E) in the Liguro-Provençal Basin (northwestern Mediterranean Sea, Figure 1). The colony is located at 28 m water depth and far from fluvial discharges. The hydrographic dynamics of this region are mainly controlled by thermohaline and wind-driven basin-wide circulation involving both the surface layer of the Modified Atlantic Water (MAW) and the underlying LIW. MAW is formed by the mixing between the North Atlantic Central Water (NACW) inflow and underlying Mediterranean Intermediate Water (MIW). The coral colony is situated at the junction of 2 water streams, both flowing northward along each side of northern Corsica. The eastern stream is part of the Tyrrhenian vein (or Eastern Corsican Current: ECC) originating from a branch of the MAW that flows counterclockwise around the Tyrrhenian Sea along Sicily and the Italian Peninsula before entering the Channel of Corsica (Pinardi et al. 2006). Its flow has a marked seasonal variability, strengthening in winter by a factor ~3 compared to summer. This is due to periodic heat losses and evaporation during the winter caused by intermittent intrusions of

$\Delta^{14}\text{C}$ Record of Surface Water in W. Mediterranean Sea

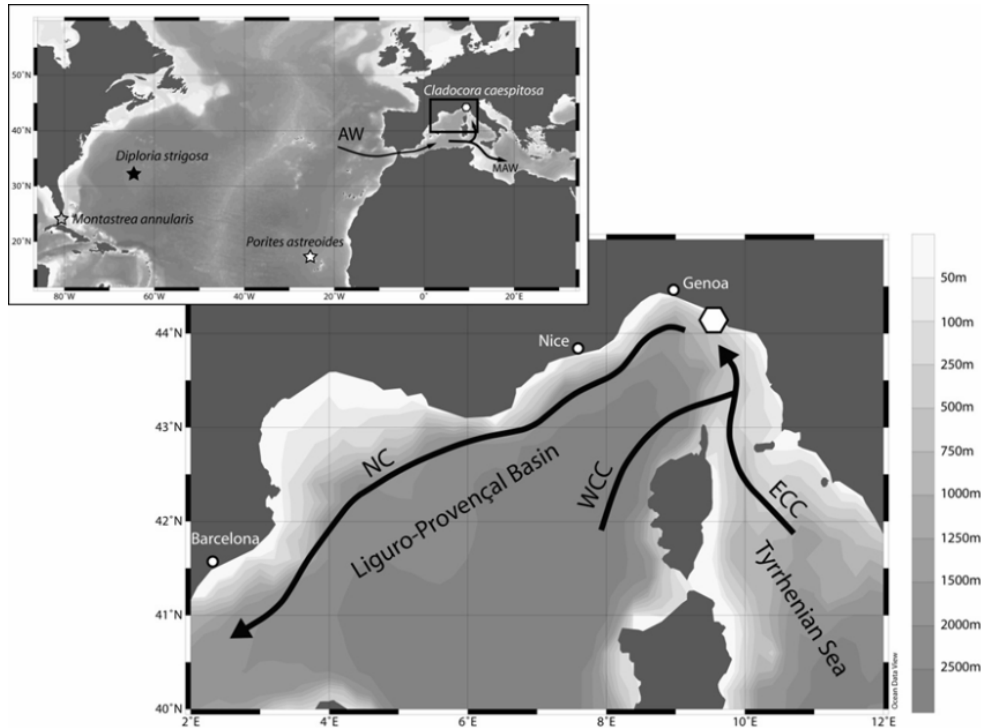


Figure 1 Map showing the location of the studied coral *Cladocora caespitosa* (white hexagon) collected alive in 1998 off the coast of Bonassola in the Liguro-Provençal Basin. Arrows represent general surface circulation pattern for the western Mediterranean Sea (WCC: Western Corsican Current; ECC: Eastern Corsican Current; NC: Northern Current). Stars indicate locations of coral sites discussed in this paper (gray star: Florida; black star: Bermuda; white star: Cape Verde). Atlantic Water (AW) and Modified Atlantic Water (MAW) are also indicated.

cold and dry northerly winds in the Ligurian Sea and the Gulf of Lions (i.e. strong Tramontana/Mistral wind events), which induce the lowering of the Ligurian-Provençal Basin steric level (Astraldi et al. 1994). The western strand (or Western Corsica Current: WCC) also displays a seasonal variability, though less pronounced than the ECC (Béthoux et al. 1982; Taupier-Letage and Millot 1986; Millot 1991). Its flow is weaker in late summer and autumn and progressively increases to a maximum in May-June and early July. The 2 currents coalesce in the north of Corsica, forming the Northern Current (also called the Liguro-Provençal-Catalan Current), which transports up to 2 Sv of seawater (Figure 1) along the slope of the Ligurian, Provençal, and Catalan coasts (Millot 1991; Sammari et al. 1995). The current is characterized by a frontal structure parallel to the coast over the shelf edge, with a width of a few tens of kilometers, a thickness of a few hundred meters, and maximum speeds of several 10 cm/s in its core (Millot and Taupier-Letage 2005). In winter, the Northern Current is composed of nearly equivalent portions from mixing of these 2 branches, whereas in summer the WCC component is predominant (Taupier-Letage and Millot 1986; Astraldi et al. 1994). The Northern Current displays large seasonal SST variations between approximately 15 °C in winter and 22 °C in summer, which are controlled by variations in the air-sea heat flux as well as in the vertical mixing and the horizontal advection of heat. In addition, the Ligurian Sea can be an area of intermediate and deep water formation during extreme meteorological conditions. Indeed, Sparnocchia et al. (1995) first showed that important convective events can occur in the Ligurian Sea regardless of the lack of topographic features that can affect the water movement.

MATERIAL AND METHOD

Coral

Cladocora caespitosa (Scleractinia, Faviidae) is the main zooxanthellate-bearing colonial coral of the Mediterranean Sea (Zibrowius 1980; Peirano et al. 2004). This species is widespread in the Mediterranean, living in coastal waters from a few meters to 40 m water depth (Morri et al. 1994). It forms subspherical colonies or large banks characterized by packets of distinct corallites, each having their own separate wall and growing in a continuous rectilinear way. The growth rate ranges from 1.3 mm/yr (Peirano et al. 1999) to 6.2 mm/yr (Kružić and Požar-Domac 2003). *C. caespitosa* shows clear annual banding with low-density bands formed in summer and high-density bands in winter (Peirano et al. 1999). During winter, coral calcification is limited to temperatures above a minimum threshold of 14–16 °C (Montagna et al. 2007). In the Ligurian Sea, seawater temperature at the depth of the coral bank (28 m) ranges from ~19 °C in summer to ~14 °C in winter (Peirano et al. 1999; Silenzi et al. 2005), indicating near continuous growth, although with a strong bias towards higher extension rates in the summer (Montagna et al. 2007).

Analytical Procedure

A 136-mm-long and 4-mm-wide corallite was extracted from the large colony. The corallite was broken into 4 pieces, cut parallel to the growth axis (Figure 2b), and analyzed for elemental concentrations by a ArF excimer 193-nm laser ablation system coupled to an inductively coupled plasma mass spectrometer (Varian 820-MS) at the Research School of Earth Sciences, Australia National University (ANU). The coral sample was scanned continuously along the thecal wall at 20 µm/s using a 20 × 200 µm rectangular slit, following the analytical method described in Montagna et al. (2007). The isotopes ⁷Li, ²⁵Mg, and ⁸⁴Sr were background-subtracted, and indexed to ⁴³Ca. Elemental concentrations were calibrated relative to pressed-powder coral standard (Davis Reef) for Mg and Sr and NIST 614 glass standard for Li. The overall analytical precision (relative standard deviation) was 4.5% for Li/Ca, 5.7% for Mg/Ca, 3.2% for Sr/Ca, and 4.3% for Li/Mg.

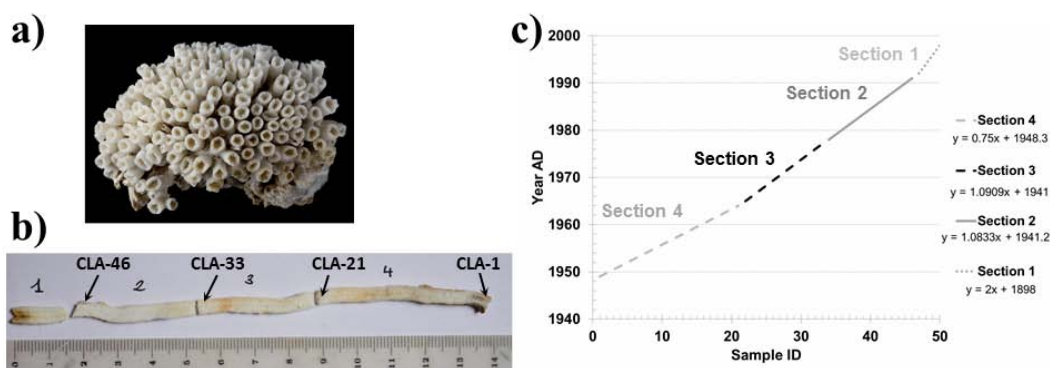


Figure 2 a) Image of a portion of the large colony of *Cladocora caespitosa* showing the typical phaceloid form (lower side of image is 9 cm). b) Corallite investigated in the present study. The 13.6-cm-long corallite was broken into 4 pieces for trace element analyses and subsampled for ¹⁴C analyses. c) The age (year AD) for each subsample was obtained by linear interpolation.

For ¹⁴C measurements, 50 subsamples (~20 mg of coral material) were collected continuously along the growth axis using a Dremel® saw. Sections 1, 2, 3, and 4 were cut into 4, 13, 12, and 21 subsamples, respectively (Figure 2b) and the coral fragments were mechanically cleaned by aluminum oxide sandblasting to remove superficial contamination, reducing the weight by ~20–30%. They were

$\Delta^{14}\text{C}$ Record of Surface Water in W. Mediterranean Sea

crushed with a mortar and pestle and the powders treated with 0.01M HNO_3 for 15 min and rinsed with Milli-QTM water to neutralize the pH. The coral aragonite was converted to CO_2 by reacting with anhydrous phosphoric acid in a semi-automated carbonate vacuum line (Tisnérat-Laborde et al. 2001). Finally, the CO_2 was reduced into graphite using hydrogen in the presence of iron powder according to the procedure developed by Arnold et al. (1989). The graphite targets were analyzed at the AMS-Artemis facility (Cottéreau et al. 2007). ^{14}C results are reported as $\Delta^{14}\text{C}$, the deviation of a sample's $^{14}\text{C}/^{12}\text{C}$ ratio from that of a pre-industrial wood standard, expressed in per mil (‰) according to the convention of Stuiver and Polach (1977), normalized to a $\delta^{13}\text{C}$ of -25.0‰ relative to the Pee Dee Belemnite (PDB) international standard, and corrected by the age of the sample and background subtraction. Background values of 0.63 ± 0.06 pMC (percent modern carbon), equivalent to an age of 41,000 yr, were obtained from the analysis of a fossil specimen *C. caespitosa* collected in an Upper Pleistocene marine deposit in southern Italy and dated by U-Th as 125,000 yr (MIS5e). Analytical precision and accuracy of ^{14}C measurements is $\pm 4\text{‰}$ at the 1σ confidence interval.

RESULTS

Chronological Framework

The phaceloid form of *C. caespitosa* consists of upward-growing individual corallites (Figure 2), making the measurement of the annual growth rate relatively straightforward compared to tropical corals with massive morphology. Peirano et al. (1999) reported growth rates between 1.30 and 4.03 mm/yr for specimens of *C. caespitosa* collected from the Ligurian Sea, with a value of 2.58 ± 0.96 mm/yr for the large colony from Bonassola, Italy. The growth rates for this species vary according to temperature-irradiance levels, being dependent on the balance of autotrophy and heterotrophy processes that regulate the rate of carbon utilized for skeleton formation (Peirano et al. 1999).

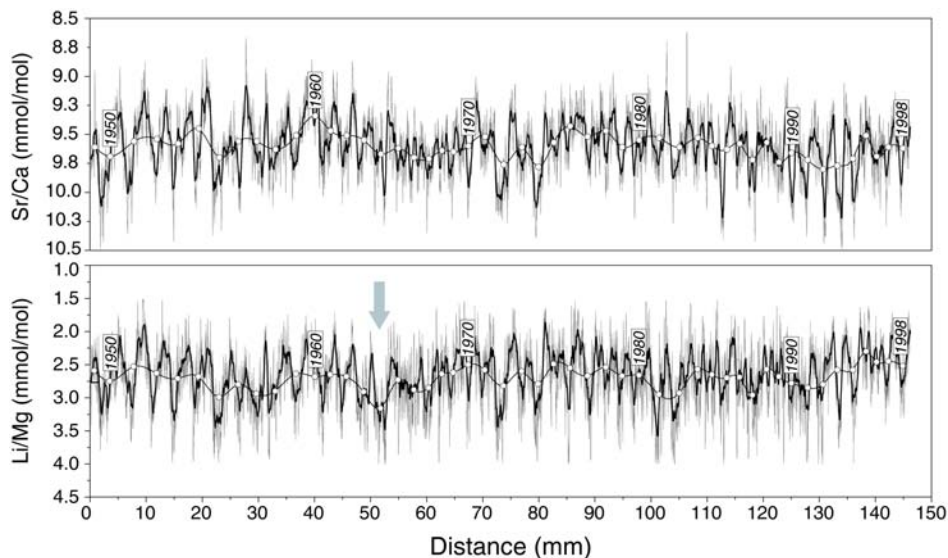


Figure 3 Sr/Ca and Li/Mg ratios measured by LA ICP-MS along the thecal wall of the corallite. The x axis represents the distance from the base of the coral (oldest part) to the coral calyx (youngest part). Note that the distance is slightly higher than the one measured in Figure 2. This is due to the fact that the corallite was not rectilinear and the laser ablation beam was focused on the thecal wall (gray line: values at 10 μm resolution; thick black line: 50-point adjacent average; thin black line with white circles: values at annual resolution). Note that the y scales are inverted. Gray arrow indicates a positive excursion in Li/Mg ratio (1963–1965) consistent with a decrease in temperatures of surface waters.

The age of the sample analyzed for ^{14}C was estimated by counting the seasonal cycles of Li/Mg and Sr/Ca ratios (Figure 3), which have been shown to be related to the seawater temperature variations (Silenzi et al. 2005; Montagna et al. 2007, 2009). Small gaps in Li/Mg and Sr/Ca ratios exist between the 4 fragments at 15.56, 55.30, and 92.98 mm from the top edge, which correspond to the positions where the corallite was broken. These gaps of $\sim 50\text{--}100\ \mu\text{m}$ do not affect the coral chronology.

Fifty distinct cycles, equivalent to 50 years' growth, were counted corresponding to an average linear growth rate of $2.72 \pm 0.59\ \text{mm/yr}$ (Figure 3), which is consistent with the value previously reported by Peirano et al. (1999) for the colony in Bonassola ($2.58 \pm 0.96\ \text{mm/yr}$). However, the annual growth is not constant along the axis with values decreasing with the age of the coral (Figure 3). To accurately define the absolute chronology for our ^{14}C subsamples, we used the year of collection (1998) combined with the number of years of each section (Figure 2) as tie points. The age of each ^{14}C subsample was further refined using linear regressions, providing a precision in the absolute age of 1 yr.

Temporal Trends in Radiocarbon

The $\Delta^{14}\text{C}$ results, plotted against time, are presented in Figure 4 (see also Table A1 in Appendix). The 50 coral subsamples cover the 50-yr period from 1949 to 1998. $\Delta^{14}\text{C}$ values range from -60‰ to 90‰ (Figure 4). The pre-bomb interval (1949–1955) has an average $\Delta^{14}\text{C}$ value of $-56 \pm 3\text{‰}$, corresponding to an age of $460 \pm 30\ \text{yr BP}$ and a reservoir age of $262 \pm 29\ \text{yr}$. The pre-bomb $\Delta^{14}\text{C}$ average agrees with previous estimates of $-54 \pm 6\text{‰}$ obtained from mollusk shells in the Liguro-Provençal area and Tyrrhenian Sea (Siani et al. 2000; Table A2 in Appendix). Two other $\Delta^{14}\text{C}$ measurements of surface seawater and mollusk shell obtained in 1956–1958 by Broecker and Gerard (1969) for the western Mediterranean basin yield a mean value of $-49 \pm 10\text{‰}$, in agreement within uncertainty with the coral value ($-39 \pm 6\text{‰}$). Additional $\Delta^{14}\text{C}$ values obtained from seawater samples in the Ionian Sea during the GEOSECS expedition in 1977 (Station 404, $35^{\circ}24'\text{N}$, $17^{\circ}12'\text{E}$, Stuiver and Östlund 1983) and 3 mollusk shells (Tisnérat-Laborde, unpublished data, Table 2A; Figure 3) match the values recorded by *C. caespitosa*, confirming the ability of this species to record seawater $\Delta^{14}\text{C}$ of DIC.

Between 1955 and 1958, $\Delta^{14}\text{C}$ values increase slightly by 5‰/yr due to a net uptake of bomb ^{14}C from the atmosphere. From 1959, the $\Delta^{14}\text{C}$ value rises at a rate of 14‰/yr until 1964. Thereafter, except for 1969 where a slight (-9‰) decrease occurred, $\Delta^{14}\text{C}$ values continue to increase, but at a lower mean rate of 6‰/yr until 1972, when a maximum value of 90‰ is reached. Afterward, $\Delta^{14}\text{C}$ values remain high, with values between $\sim 52\text{‰}$ and $\sim 85\text{‰}$ and exhibit a negative fluctuating trend until the end of the record in 1998. Spectral analysis of the post-bomb data does not show any clear periodicity. However, slight decreases are observed in 1969, 1973–1974, 1976–1977, 1980, and 1989 with variations in amplitude ranging from 9 to 18‰ (Figure 4).

DISCUSSION

Pre-Bomb $\Delta^{14}\text{C}$ Signature

The WMS pre-bomb (1949–1955) $\Delta^{14}\text{C}$ record yields a mean value of $-56 \pm 3\text{‰}$, similar to the signature of the northeast Atlantic (NEA) surface estimated at $-57 \pm 7\text{‰}$ between 1948 and 1952 (Tisnérat-Laborde et al. 2010). This similarity reflects the oceanic circulation pattern with North Atlantic Central Water (NACW) entering the Mediterranean Sea as a surface flow through the Strait of Gibraltar. Atlantic Water flows to the northwestern and eastern Mediterranean basins and is gradually transformed into Modified Atlantic Water by mixing with upwelled Mediterranean Intermediate

$\Delta^{14}\text{C}$ Record of Surface Water in W. Mediterranean Sea

Water (MIW). In contrast to SST, salinity, and heat transfer, which are modified along the Strait of Gibraltar due to the interaction with the atmosphere and mixing with intermediate waters (Millot and Taupier-Letage 2005), the $\Delta^{14}\text{C}$ signature of NACW inflow does not change compared to MSW. Indeed, Intermediate waters in western Mediterranean Sea have a $\Delta^{14}\text{C}$ signature of about $-55 \pm 16\text{‰}$, similar to surface waters of the western Mediterranean Sea reflecting the rapid turnover time of $\sim 70\text{--}100$ yr (Broecker and Gerard 1969; Siani et al. 2001; McCulloch et al. 2010). Consequently, although mixing between surface and intermediate waters occurs, the insignificant $\Delta^{14}\text{C}$ gradient between those water masses results in similar $\Delta^{14}\text{C}$ signature between the western Mediterranean Sea and the incoming Atlantic Water, confirming the important link between the Mediterranean and the Atlantic.

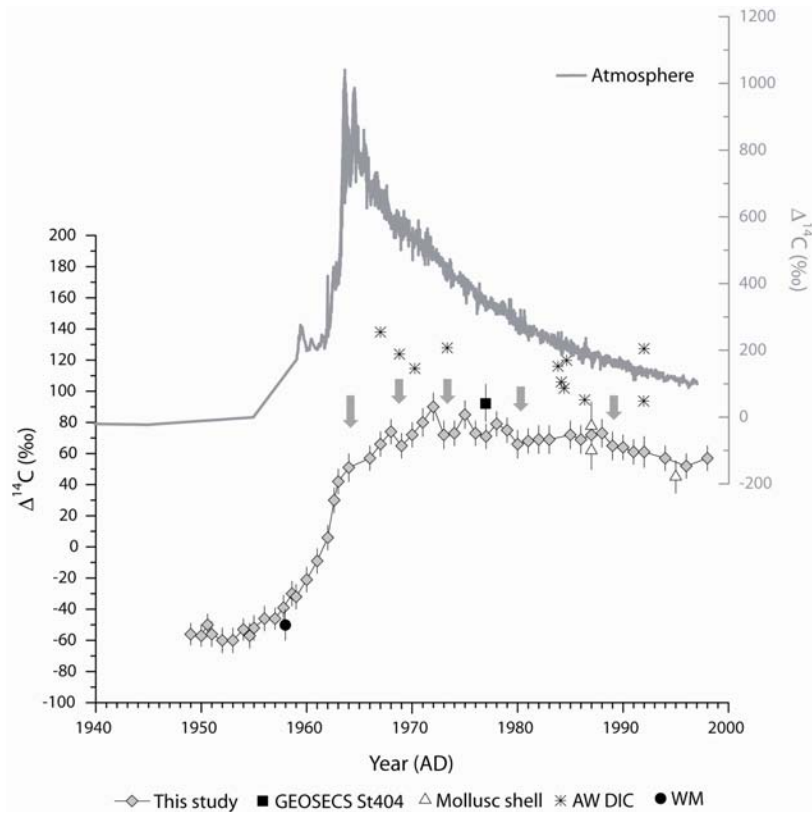


Figure 4 The coral-based $\Delta^{14}\text{C}$ values (gray diamonds) for the western Mediterranean Sea are plotted against time (year AD). Also shown are atmospheric $\Delta^{14}\text{C}$ values from a compilation of tree-ring records (Stuiver et al. 1998) and $^{14}\text{CO}_2$ measurements in Northern Hemisphere (Levin et al. 1995), $\Delta^{14}\text{C}$ values from western Mediterranean mollusks (white triangles, Tisnérat-Laborde, unpublished), surface seawater $\Delta^{14}\text{C}$ measurements from GEOSECS Station 404 (black square, Stuiver and Östlund 1983) and from the Western Basin (black circle, Broecker and Gerard 1969) and North Central Atlantic Water DIC $\Delta^{14}\text{C}$ measurements (black crosses, Nydal and Gislefoss 1996). Vertical bars represent 2σ errors. The gray arrows indicate the $\Delta^{14}\text{C}$ drops discussed in the text.

The -56‰ pre-bomb mean $\Delta^{14}\text{C}$ value of the western Mediterranean and NEA has an offset of $\sim 12\text{‰}$ when compared to the one derived for the northwest Atlantic from Bermuda corals (-45‰ ; Druffel 1987). This offset is related to the arrival of depleted waters in the NEA. In a recent study,

Tisnérat-Laborde et al. (2010) showed that NEA surface waters result from a mixture of subtropical (Bermuda ^{14}C signature) and subpolar mode waters, the latter being the upstream source of the ^{14}C -depleted Labrador Sea. This mixing leads to lower $\Delta^{14}\text{C}$ values for the NEA and, consequently, for the Mediterranean Sea compared to Bermuda waters.

Uptake of Bomb Radiocarbon in Mediterranean Sea

Our results show an initial rapid uptake of bomb ^{14}C for the period 1953–1963 corresponding to the fast atmospheric $\Delta^{14}\text{C}$ rise globally (Levin et al. 1995; Levin and Kromer 1997; Nydal and Gislefoss 1996) (Figure 4). The comparison between the Mediterranean, Florida, and Bermuda $\Delta^{14}\text{C}$ records reveals similar uptake rates for this period with a significant correlation ($r = 0.98$) between the WMS and Florida. The timing of the post-bomb $\Delta^{14}\text{C}$ peak is consistent with the estimated $^{14}\text{CO}_2$ time transfer (~ 10 yr) from the atmosphere to the ocean (Broecker and Peng 1982).

After 1963, a significant difference between WMS and NW Atlantic (Florida and Bermuda) $\Delta^{14}\text{C}$ signals appears. $\Delta^{14}\text{C}$ values in the North Atlantic exceed $\sim 150\text{‰}$ (except for Cape Verde; Druffel 1996), whereas those for the WMS are $\sim 90\text{‰}$. The different magnitudes of the post-bomb $\Delta^{14}\text{C}$ peak cannot be explained by a change of air-sea $^{14}\text{CO}_2$ exchange. Indeed, the $^{14}\text{CO}_2$ flux to and from the ocean is primarily proportional to the difference between the partial pressures of the sea surface and the atmosphere. During 1963–1972, the ^{14}C concentration in the atmosphere was very high ($>470\text{‰}$) and similar for all these locations. The large gradient between atmosphere and ocean causes a systematic ^{14}C flux from the atmosphere to the ocean. Secondly, the flux is proportional to the temperature-dependent solubility and the gas-exchange coefficient (or piston velocity), which is a function of wind speed. However, both oceanic regions are characterized by predominantly westerly winds and by similar annual subtropical temperature regimes (Levitus and Boyer 1994). Given that surface WMS is strongly dominated by Atlantic inflow, such atmospheric forcing factors should cause small annual differences between both oceanic regions. Hence, other reasons besides CO_2 gas exchange rates must account for the observed difference of almost 60‰.

Differences regarding the amplitude and attenuation of the post-bomb $\Delta^{14}\text{C}$ peak are more likely indicative of oceanic mixing processes such as the contribution of ^{14}C -depleted subsurface waters into the surface layers. Such a process is recorded at Cape Verde (Figure 5), with significantly lower bomb ^{14}C amplitude of $60 \pm 10\text{‰}$ (Druffel 1996). Here, the surface waters are influenced by the input of the North Equatorial Current, which is depleted in ^{14}C by the influence of the Mauritanian upwelling of ^{14}C -depleted intermediate and deep waters (Druffel 1996).

In Mediterranean Sea Water (MSW), the arrival of depleted water may be derived from local ocean processes as vertical mixing or large-scale ocean circulation since the sampling site is influenced by the WCC and ECC. As discussed previously, these waters originate from Modified Atlantic Water being formed by the mixing between the North Atlantic Central Water inflow and underlying Mediterranean Intermediate Water and the Levantine Intermediate Water (Millot and Taupier-Letage 2005). The ^{14}C observations of AW performed during hydrographic campaigns (Station 12; Nydal et al. 1984; Atlantis II-78, Fairhall and Young 1985; and Station 90; Severinghaus et al. 1996) between 1967 and 1992 provide some constraints on the evolution of $\Delta^{14}\text{C}$ signature of Atlantic Ocean inflow. These $\Delta^{14}\text{C}$ values are systematically higher ($>95\text{‰}$) than those of MSW (Figure 4), indicating that the addition of ^{14}C -depleted water occurs in the Mediterranean Sea and not in the North Atlantic Central Water prior to its inflow.

As already noted, AW inflow mixes with underlying Mediterranean waters due to a density increase through evaporation, particularly during winter when air is dry and cold (Millot and Taupier-Letage

$\Delta^{14}\text{C}$ Record of Surface Water in W. Mediterranean Sea

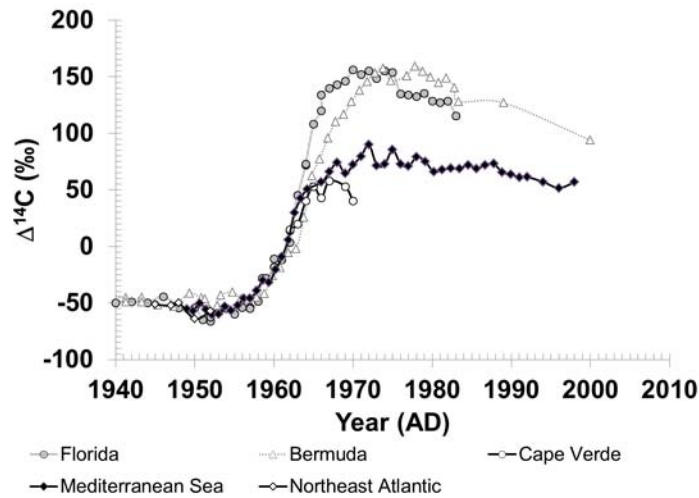


Figure 5 Western Mediterranean Sea and North Atlantic $\Delta^{14}\text{C}$ time series. A comparison between the Mediterranean, Florida, and Bermuda records reveals similar bomb- ^{14}C uptake rates for the period 1953–1963, corresponding to the fast atmospheric $\Delta^{14}\text{C}$ rise globally. After 1963, significant $\Delta^{14}\text{C}$ differences appear between WMS and North Western Atlantic signals, with the WMS showing lower $\Delta^{14}\text{C}$ values. This difference is likely related to water mass mixing processes in the Mediterranean, such as the contribution of ^{14}C -depleted subsurface waters into the surface layers.

2005). During the post-bomb period, a large gradient of $\Delta^{14}\text{C}$ exists between surface ^{14}C waters already enriched by bomb ^{14}C and low $\Delta^{14}\text{C}$ intermediate waters (-60% , Broecker and Gerard 1969; -50% , McCulloch et al. 2010) and continues over several years as shown in the GEOSECS depth ^{14}C profile (-60% , Stuiver and Östlund 1983). Consequently, the lower overall values of the bomb $\Delta^{14}\text{C}$ peak observed in WMS surface water can be attributed to vertical mixing and equilibration with the depleted subsurface and intermediate waters. Synchronous with the change of the $\Delta^{14}\text{C}$ slope of WMS, a significantly lower temperature is observed in 1963 based on the Li/Mg ratio, which is used here as a reliable temperature proxy (Montagna et al. 2009; Case et al. 2010) (Figure 3). This temperature decrease is also observed in the surface western Mediterranean during the same period (Sahsamanoglou and Makrogiannis 1992). Furthermore, several studies on climatic variations in the Mediterranean Sea noted that a change of mean climate state began in 1960 with an increase in atmospheric pressure (Makrogiannis and Sahsamanoglou 1990). This increase is attributed to the change in atmospheric circulation from positive to negative NAO phase (1960–1967) with an associated southward shift of the storm track causing colder winter temperatures for western Europe in 1963 (Cattiaux et al. 2011). The SST decrease linked to this condition is likely to promote more mixing that can explain the rapid change of the $\Delta^{14}\text{C}$ slope of MSW in 1964 and the further lower increase rate until 1972. ,

Using a simple 2-endmember mixing model we tested the hypothesis that variable vertical mixing of MAW and LIW could be at the origin of bomb ^{14}C increase change noted beyond 1963 and the largely attenuated bomb ^{14}C peak. Figure 6 summarizes this model. Here, we initiate the model with the hypothesis that $\Delta^{14}\text{C}$ values in LIW are -50% in 1955 and slowly evolve towards values of $\sim 0\%$ in 1990 due to continuous entrainment of bomb ^{14}C surface water at depth (see Appendix). On the contrary, AW entering the Mediterranean Sea is supposed to contain slightly less ^{14}C compared to the west Atlantic as indicated by the difference between the coral record from Florida and the sparse seawater measurements. Assuming that the WMS water is a mixture of both AW and LIW, one

obtains a mixing ratio of ~80 and ~20%, respectively, for the period 1958–1964, during which both the WMS and northern Atlantic increase at equal $\Delta^{14}\text{C}$ rates. Beyond 1964, our simplistic model requires a stronger entrainment of LIW to the surface, leading to a rate of ~70/30% AW/LIW until 1990. Our model indicates a potential decadal change of variability for the exchange of AW and LIW. When we compared the mixing ratio with the NAO winter index, we observed a good correlation with a delay of 3 yr (Figure 6), indicating a link between increased mixing observed with ^{14}C and atmospheric conditions. However, further investigations are necessary to identify whether the mixture of AW and LIW is related to vertical mixing due to convective processes or enhanced upwelling involving the 2 layers, which occurs in the northern Tyrrhenian basin (Artale et al. 1994; Astraldi et al. 1994).

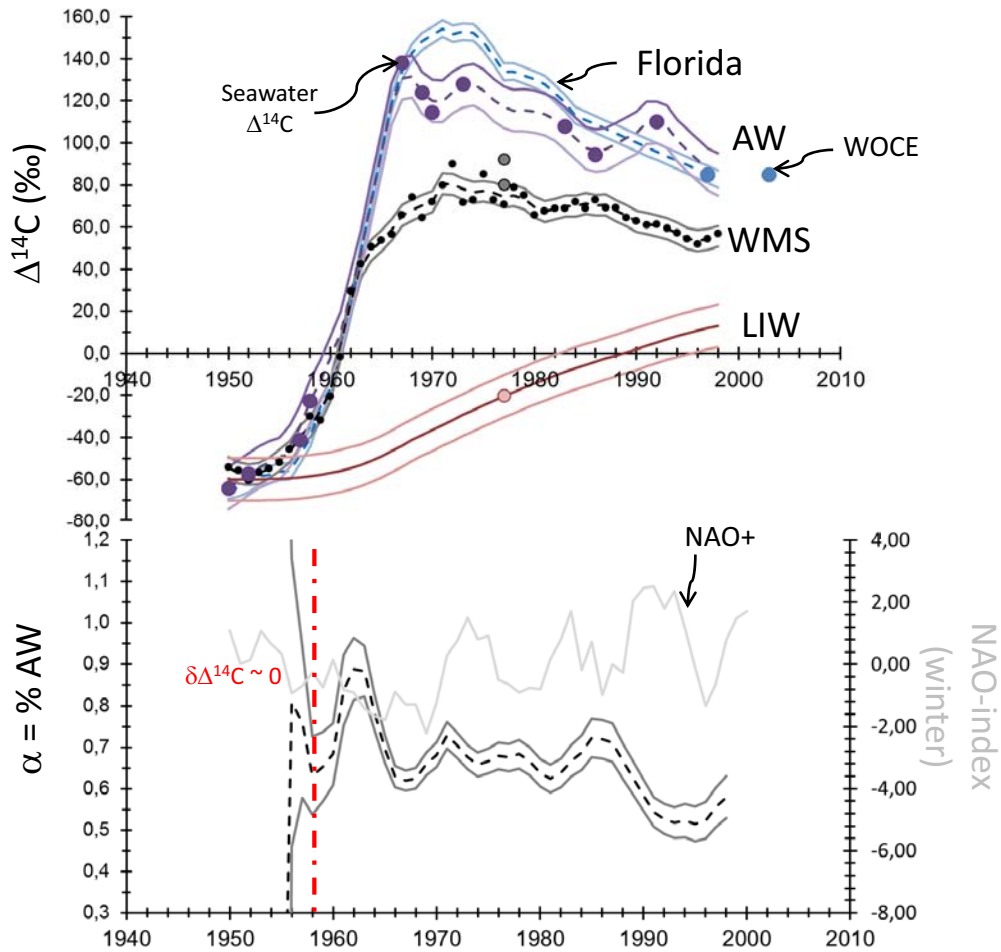


Figure 6 Top panel: 3-yr running average $\Delta^{14}\text{C}$ records for Florida coral (light blue lines), WMS coral (black lines), Atlantic inflow (violet lines), and Levantine Intermediate water (red lines). Atlantic inflow and LIW records are estimates based on punctuated seawater measurements and using assumptions on the shape (Atlantic) and turnover rate (Mediterranean Sea). Dots correspond to punctuated seawater measurements respective of the water masses exchanging at the WMS coral site. Lower panel: Percentage of Atlantic inflow (α) as derived from a simplistic 2-endmember mixing calculation ($\alpha = (\Delta^{14}\text{C}_{\text{WMS}} - \Delta^{14}\text{C}_{\text{LIW}}) / (\Delta^{14}\text{C}_{\text{AI}} - \Delta^{14}\text{C}_{\text{LIW}})$). Prior to 1959, this calculation is not valid due to the missing ^{14}C gradient between mixing water masses. Beyond 1990, the mixing calculation is very sensitive to the presumed ^{14}C evolution of LIW and is thus not further considered. Finally, the mass balance estimate is compared to the winter NAO index.

$\Delta^{14}\text{C}$ Record of Surface Water in W. Mediterranean Sea

After the bomb peak in 1972, the $\Delta^{14}\text{C}$ record begins a slow decrease until 1998 due to a declining gradient in ^{14}C between atmosphere and surface ocean as well as ongoing dilution of surface water with intermediate and deep waters. Fluctuations of post-bomb $\Delta^{14}\text{C}$ values are related to oceanic dynamics and not likely to air-sea gas exchange because of the large impedance for CO_2 exchange at the air-sea interface (Druffel 1996) although they are derived from changes in local or basin ocean dynamics, which are closely linked to atmospheric conditions. Sparnocchia et al. (1995) indicated that in 1968 a violent storm associated with strong cold winds caused mixing and cooling of the water column to a depth of 1200 m in the Ligurian Sea. The first $\Delta^{14}\text{C}$ drop in 1969 may be explained by this rapid vertical mixing. The rapidity of this event (8 days) may account for the lack of changes in sea temperature being recorded by Li/Mg. This result suggests that the rapid decreases of $\Delta^{14}\text{C}$ in 1972–1973, 1980, and 1989 can also be associated with similar oceanic processes, although no hydrological data are available to confirm this.

CONCLUSION

This study presents the first annually resolved $\Delta^{14}\text{C}$ time series of the surface western Mediterranean Sea for the period 1949–1998, derived from a long-lived specimen of the zooxanthellate coral *Cladocora caespitosa* collected in the Ligurian Sea in 1998. We show that measurement of the seasonal cycles using Sr/Ca and Li/Mg ratios provides an accurate estimate of the age of the coral. The $\Delta^{14}\text{C}$ average of the pre-bomb surface waters is $-56 \pm 3\text{‰}$, corresponding to an age of 460 ± 30 yr BP and a reservoir age of 262 ± 29 yr. The uptake of bomb ^{14}C is revealed by a steady increase after 1955 with $\Delta^{14}\text{C}$ values rising rapidly until 1964, similarly to those from corals in the northern Atlantic. While North Atlantic $\Delta^{14}\text{C}$ values continue to increase until 1967, the Mediterranean record shows a slower rate rise to a lower maximum value of $90 \pm 5\text{‰}$ that is reached in 1972. We associate this difference to a change from positive to negative NAO phase that implies an increase of mixing of surface waters with ^{14}C -depleted subsurface and intermediate waters that occurred at the scale of the whole western basin of the Mediterranean Sea. Following this event, the post-bomb ^{14}C pattern shows relatively minor fluctuations that are attributed to changes in local vertical mixing.

ACKNOWLEDGMENTS

We gratefully acknowledge M Paterne, E Douville, and C Hatté for helpful comments and discussions. We thank C Noury and the other members of the ^{14}C laboratory (LSCE) who helped us to treat samples. We thank C Moreau and the staff of the AMS-Artemis facility (UMS 2572) who measured ^{14}C . P Montagna is grateful for financial support from the Marie Curie International Outgoing Fellowship (MEDAT-ARCHIVES). This work was supported by the MISTRALS/PALEOMEX/COFIMED project, funded by the French CNRS, the CEA, and the ARC Centre of Excellence in Coral Reef Studies. This study is dedicated to the memory of our colleague Sergio Silenzi, who sadly passed away in 2012. This is LSCE contribution n°4555 and ISMAR contribution n°1788.

REFERENCES

- Arnold M, Bard E, Maurice P, Valladas H, Duplessy JC. 1989. ^{14}C dating with the Gif-sur-Yvette Tandem accelerator: status report and study of isotopic fractionation in the sputter ion source. *Radiocarbon* 31(3): 284–91.
- Artale V, Astraldi M, Buffoni G, Gasparini GP. 1994. The seasonal variability of the gyre-scale circulation in the northern Tyrrhenian Sea. *Journal of Geophysical Research* 99(C7):14,127–37.
- Astraldi M, Gasparini GP, Sparnocchia S. 1994. The seasonal and interannual variability in the Ligurian-Provencal Basin. *Coastal and Estuarine Studies* 46: 93–113.
- Barnston AG, Livezey RE. 1987. Classification, seasonality and persistence of low-frequency atmospheric circulation patterns. *Monthly Weather Review* 115: 1083–126.
- Belkin M. 2009. Rapid warming of large marine ecosystems.

- tems. *Progress in Oceanography* 81:207–13.
- Béthoux JP, Prieur L, Nyffeler F. 1982. The water circulation in the North-Western Mediterranean Sea, its relation with wind and atmospheric pressure. In: Nihoul JC, editor. *Hydrodynamics of Semi Enclosed Seas*. Elsevier Oceanography Series 34. p 129–42.
- Broecker WS, Gerard R. 1969. Natural radiocarbon in the Mediterranean Sea. *Limnology and Oceanography* 14:883–8.
- Broecker WS, Peng TH. 1982. *Tracers in the Sea*. Palisades: Lamont-Doherty Geological Observatory.
- Broecker WS, Peng TH, Östlund HG, Stuiver M. 1985. The distribution of bomb radiocarbon in the ocean. *Journal of Geophysical Research* 90(C4):6953–70.
- Campana SE. 1997. Use of radiocarbon from nuclear fallout as a dated marker in the otoliths of haddock *Melanogrammus aeglefinus*. *Marine Ecology Progress Series* 150:49–56.
- Case DH, Robinson LF, Auro ME, Gagnon AC. 2010. Environmental and biological controls on Mg and Li in deep-sea scleractinian corals. *Earth and Planetary Science Letters* 300:215–25.
- Cattiaux J, Vautard R, Yiou P. 2011. North-Atlantic SST amplified recent wintertime european land temperature extremes and trends. *Climate Dynamics* 36:2113–28.
- Cember R. 1989. Bomb radiocarbon in the Red Sea: a medium-scale gas exchange experiment. *Journal of Geophysical Research* 94(C2):2111–23.
- Cottreau E, Arnold M, Moreau C, Baqué D, Bavay D, Caffy I, Comby C, Dumoulin JP, Hain S, Perron M, Salomon J, Setti V. 2007. Artemis, the new ¹⁴C AMS at LMC14 in Saclay, France. *Radiocarbon* 49(2):291–9.
- Druffel ERM. 1987. Bomb radiocarbon in the Pacific: annual and seasonal timescale variations. *Journal of Marine Research* 45(3):667–98.
- Druffel ERM. 1989. Decade time scale variability of ventilation in the North Atlantic: high-precision measurements of bomb radiocarbon in banded corals. *Journal of Geophysical Research* 94(C3):3271–85.
- Druffel ERM. 1996. Post-bomb radiocarbon records of surface corals from the tropical Atlantic Ocean. *Radiocarbon* 38(3):563–72.
- Druffel ERM, Griffin S. 1993. Large variations of surface ocean radiocarbon: evidence of circulation changes in the southwestern Pacific. *Journal of Geophysical Research* 98(C11):20,249–59.
- Druffel ERM, Griffin S. 1999. Variability of surface ocean radiocarbon and stable isotopes in the southwestern Pacific. *Journal of Geophysical Research* 104(C10):23,607–13.
- Druffel ERM, Linick TW. 1978. Radiocarbon in annual coral rings of Florida. *Geophysical Research Letters* 5(11):913–6.
- Druffel ERM, Griffin S, Guilderson TP, Kashgarian M, Southon J, Schrag DP. 2001. Changes of subtropical North Pacific radiocarbon and correlation with climate variability. *Radiocarbon* 43(1):15–25.
- Fairhall AW, Young AW. 1985. Historical ¹⁴C measurements from the Atlantic, Pacific, and Indian oceans. *Radiocarbon* 27(3):473–507.
- Fallon SJ, Guilderson TP. 2008. Surface water processes in the Indonesian throughflow as documented by a high-resolution coral $\Delta^{14}\text{C}$ record. *Journal of Geophysical Research* 113:C09001, doi:10.1029/2008JC004722.
- Guilderson TP, Schrag DP. 1998. Abrupt shift in subsurface temperatures in the tropical Pacific associated with changes in El Niño. *Science* 281(5374):240–3.
- Guilderson T, Caldeira K, Duffy PB. 2000a. Radiocarbon as a diagnostic tracer in ocean and carbon cycle modeling. *Global Biogeochemical Cycles* 14(3):887–902.
- Guilderson TP, Schrag DP, Goddard E, Kashgarian M, Wellington GM, Linsley BK. 2000b. Southwest subtropical pacific surface water radiocarbon in a high-resolution coral record. *Radiocarbon* 42(2):249–56.
- Guilderson TP, Fallon S, Moore MD, Schrag DP, Charles CD. 2009. Seasonally resolved surface $\Delta^{14}\text{C}$ variability in the Lombok Strait: a coralline perspective. *Journal of Geophysical Research* 114: C07029, doi: 10.1029/2008JC004876.
- Hurrell JW, Deser C. 2009. Atlantic climate variability: the role of the North Atlantic Oscillation. *Journal of Marine Systems* 78(1):28–41.
- Hurrell JW, Kushnir Y, Ottersen G, Visbeck M. 2003. An overview of the North Atlantic Oscillation: climatic significance and environmental impact. *Geophysical Monograph American Geophysical Union* 134:1–35.
- Josey SA, Somot S, Tsimplis M. 2011. Impacts of atmospheric modes of variability on Mediterranean Sea surface heat exchange. *Journal of Geophysical Research* 116: C02032, doi:10.1029/2010JC006685.
- Kalish JM, Nydal R, Nedreaas KH, Burr GS, Eine GL. 2001. A time history of pre- and post-bomb radiocarbon in the Barents Sea derived from Arcto-Norwegian cod otoliths. *Radiocarbon* 43(2B):843–55.
- Konishi K, Tanaka T, Sakanoue M. 1982. Secular variation of radiocarbon concentration in sea water: sclerochronological approach. Presented at the *Fourth International Coral Reef Symposium*.
- Kružić P, Požar-Domac A. 2003. Banks of the coral *Cladocora caespitosa* (Anthozoa, Scleractinia) in the Adriatic Sea. *Coral Reefs* 22:536.
- Levin I, Kromer B. 1997. Twenty years of atmospheric ¹⁴CO₂ observations at Schauinsland station, Germany. *Radiocarbon* 39(2):205–18.
- Levin I, Graul R, Trivett NBA. 1995. Long-term observation of atmospheric CO₂ and carbon isotopes at continental sites in Germany. *Tellus B* 47(1–2):23–34.
- Levitus S, Boyer TP. 1994. *World Ocean Atlas 1994. Volume 4, Temperature, NAOO Atlas NESDIS*. Silver Springs: National Oceanic and Atmospheric Administration. 129 p.

$\Delta^{14}\text{C}$ Record of Surface Water in W. Mediterranean Sea

- Makrogiannis TJ, Sahsamanoglou HS. 1990. Time variation of the mean sea level pressure over the major Mediterranean area. *Theoretical and Applied Climatology* 41:149–56.
- McCulloch M, Taviani M, Montagna P, Lopez-Correa M, Remia A, Mortimer G. 2010. Proliferation and demise of deep-sea corals in the Mediterranean during the Younger Dryas. *Earth and Planetary Science Letters* 298:143–52.
- Millot C. 1991. Mesoscale and seasonal variabilities of the circulation in the western Mediterranean. *Dynamics of Atmospheres and Oceans* 15:179–214.
- Millot C, Taupier-Letage I. 2005. Circulation in the Mediterranean Sea. *The Handbook of Environmental Chemistry* 5(K):26–66, doi:10.1007/b107143.
- Montagna P, McCulloch M, Mazzoli C, Silenzi S, Odorico. 2007. The non-tropical coral *Cladocora caespitosa* as the new climate archive for the Mediterranean: high-resolution (~weekly) trace element systematics. *Quaternary Science Reviews* 26:441–62.
- Montagna P, Silenzi S, Devoti S, Mazzoli C, McCulloch M, Scicchitano G, Taviani M. 2008. Climate reconstructions and monitoring in the Mediterranean Sea: A review on some recently discovered high-resolution marine archives. *Rendiconti Lincei* 19:121–40.
- Montagna P, López Correa M, Rüggeberg A, McCulloch M, Rodolfo-Metalpa R, Ferrier-Pagès C, Freiwald A, Goldstein S, Henderson G, Mazzoli C, Russo S, Silenzi S, Taviani M, Trotter J. 2009. Li/Mg ratios in shallow and deep-sea coral exoskeleton as a new temperature proxy. Presented at the AGU Fall Meeting, 14–18 December 2009, San Francisco, USA.
- Morri C, Peirano A, Bianchi CN, Sassarini M. 1994. Present-day bioconstructions of the hard coral, *Cladocora caespitosa* (L.) (Anthozoa, Scleractinia), in the eastern Ligurian Sea (NW Mediterranean). *Biologia Marina Mediterranea* 1:371–2.
- Nozaki Y, Rye DM, Turekian KK, Dodge RE. 1978. A 200 year record of carbon-13 and carbon-14 variations in a Bermuda coral. *Geophysical Research Letters* 5(10):825–8.
- Nydal R, Gislefoss JS. 1996. Further application of bomb ^{14}C as a tracer in the atmosphere and ocean. *Radiocarbon* 38(3):389–406.
- Nydal R, Gulliksen S, Lövseth K, Skogseth F. 1984. Bomb ^{14}C in the ocean surface 1966–1981. *Radiocarbon* 26(1):7–45.
- Papadopoulos V, Josey SA, Bartzokas A, Somot S, Ruiz S, Drakopoulou P. 2012. Large-scale atmospheric circulation favoring deep- and intermediate-water formation in the Mediterranean Sea. *Journal of Climate* 25(18):6079–91.
- Peirano A, Morri C, Bianchi CN. 1999. Skeleton growth and density pattern of the temperate, zooxanthellate scleractinian *Cladocora caespitosa* from the Ligurian Sea (NW Mediterranean). *Marine Ecology Progress Series* 185:195–201.
- Peirano A, Morri C, Bianchi CN, Aguirre J, Antonioli F, Calzetta G, Carobene L, Mastronuzzi G, Orrù P. 2004. The Mediterranean coral *Cladocora caespitosa*: a proxy for past climate fluctuations? *Global and Planetary Change* 40:195–200.
- Pinardi N, Arneri E, Crise A, Ravaoli M, Zavatarelli M. 2006. The physical, sedimentary and ecological structure and variability of shelf areas in the Mediterranean Sea. In: Robinson AR, Brink K, editors. *The Sea*. Cambridge: Harvard University Press. p 1243–330.
- Reimer PJ, McCormac FG. 2002. Marine radiocarbon reservoir corrections for the Mediterranean and Aegean Seas. *Radiocarbon* 44(1):159–66.
- Reimer PJ, Baillie MGL, Bard E, Bayliss A, Beck WJ, Bertrand C, Blackwell PG, Buck CE, Burr GS, Cutler KB, Damon PE, Edwards RL, Fairbanks RG, Friedrich M, Guilderson TP, Hughen KA, Kromer B, McCormac FG, Manning S, Bronk Ramsey C, Reimer RW, Remmele S, Southon JR, Stuiver M, Talamo S, Taylor FW, van der Plicht J, Weyhenmeyer CE. 2004a. IntCal04 terrestrial radiocarbon age calibration, 0–26 cal kyr BP. *Radiocarbon* 46(3):1029–58.
- Rixen M, Beckers JM, Levitus S, Antonov J, Boyer T, Maillard C, Fichaut M, Balopoulos E, Iona S, Dooley H, Garcia MJ, Manca B, Giorgetti A, Manzella G, Mikhailov N, Pinardi N, Zavatarelli. 2005. The western Mediterranean deep water: a proxy for climate change. *Geophysical Research Letters* 32: L12608, doi:10.1029/2005GL022702.
- Rodgers KB, Aumont O, Madec G, Menkes C, Blanke B, Monfray P, Orr JC, Schrag DP. 2004. Radiocarbon as a thermocline proxy for the eastern equatorial Pacific. *Geophysical Research Letters* 31(14): L14314, doi: 10.1029/2004GLO19764.
- Sahsamanoglou HS, Makrogiannis TJ. 1992. Temperature trends over the Mediterranean region, 1950–88. *Theoretical and Applied Climatology* 45:183–92.
- Sammari C, Millot C, Prieur L. 1995. Aspects of the seasonal and mesoscale variabilities of the Northern current in the western Mediterranean Sea inferred from the PROLIG-2 and PROS-6 experiments. *Deep-Sea Research I* 42(6):893–917.
- Severinghaus JP, Broecker WS, Peng TH, Bonani G. 1996. Transect along 24°N latitude of ^{14}C in dissolved inorganic carbon in the subtropical North Atlantic ocean. *Radiocarbon* 38(3):407–14.
- Sherwood OA, Edinger EN, Guilderson TP, Ghaleb B, Risk M, Scott DB. 2008. Late Holocene radiocarbon variability in Northwest Atlantic slope waters. *Earth and Planetary Science Letters* 275:146–53.
- Siani G, Paterne M, Arnold M, Bard E, Metivier B, Tisnérat N, Bassinot F. 2000. Radiocarbon reservoir ages in the Mediterranean Sea and Black Sea. *Radiocarbon* 42(2):271–80.
- Siani G, Paterne M, Michel E, Sulpizio R, Sbrana A, Arnold M, Haddad G. 2001. Mediterranean Sea surface radiocarbon reservoir age changes since the last gla-

- cial maximum. *Science* 294(5548):1917–20.
- Silenzi S, Bard E, Montagna P, Antonioli F. 2005. Isotopic records in a non-topical coral (*Cladocora caespitosa*) from the Mediterranean Sea: evidence of a new high-resolution climate archive. *Global and Planetary Change* 49:94–120.
- Sparnocchia S, Picco P, Manzella G, Ribotti A, Copello S, Brasey P. 1995. Intermediate water formation in the Ligurian Sea. *Oceanologica Acta* 18(2):151–62.
- Stuiver M, Östlund HG. 1983. GEOSECS Indian Ocean and Mediterranean radiocarbon. *Radiocarbon* 25(1):1–29.
- Stuiver M, Polach HA. 1977. Discussion: reporting of ^{14}C data. *Radiocarbon* 19(3):355–63.
- Stuiver M, Reimer PJ, Bard E, Beck JW, Burr GS, Hughen KA, Kromer B, McCormac G, van der Plicht J, Spurk M. 1998. INTCAL98 radiocarbon age calibration, 24,000–0 cal BP *Radiocarbon* 40(3):1041–83.
- Taupier-Letage I, Millot C. 1986. General hydrodynamical features in the Ligurian Sea inferred from the DY-OME experiment. *Oceanologica Acta* 9:119–31.
- Tisnérat-Laborde N. 2010. Variations du $\Delta^{14}\text{C}$ dans l'océan de surface de l'Atlantique Nord-est au cours des 200 dernières années [PhD thesis]. Université Paris-Sud XI, Orsay, France. 189 p.
- Tisnérat-Laborde N, Poupeau JJ, Tannau JF, Paterne M. 2001. Development of a semi-automated system for routine preparation of carbonate sample. *Radiocarbon* 43(2A):299–304.
- Tisnérat-Laborde N, Paterne M, Métivier B, Arnold M, Yiou P, Blamart D, Raynaud S. 2010. Variability of the northeast Atlantic sea surface $\Delta^{14}\text{C}$ and marine reservoir age and the North Atlantic Oscillation (NAO). *Quaternary Science Reviews* 29:2633–46.
- Toggweiler JR, Dixon K, Bryan K. 1989. Simulations of radiocarbon in a coarse-resolution world ocean model 1. Steady state prebomb distributions. *Journal of Geophysical Research* 94(C6):8217–64.
- Toggweiler JR, Dixon K, Broecker WS. 1991. The Peru upwelling and ventilation of the South Pacific thermocline. *Journal of Geophysical Research* 96(C11):20,467–97.
- Trigo IF, Bigg GR, Davies TD. 2002. Climatology of cyclogenesis mechanisms in the Mediterranean. *Monthly Weather Review* 130:549–69.
- Trotter J, Montagna P, McCulloch M, Silenzi S, Reynaud S, Mortimer G, Martin S, Ferrier-Pagès C, Gattuso JP, Rodolfo-Metalpa R. 2011. Quantifying the pH 'vital effect' in the temperate zooxanthellate coral *Cladocora caespitosa*: validation of the boron seawater pH proxy. *Earth and Planetary Science Letters* 303:163–73.
- Weidman CR, Jones GA. 1993. A shell-derived time history of bomb ^{14}C on Georges Bank and its Labrador Sea implications. *Journal of Geophysical Research* 98(C8):14,577–88.
- Zibrowius H. 1980. Les Scléactiniaires de la Méditerranée et de l'Atlantique nord-oriental. *Mémoires de l'Institut Océanographique (Monaco)* 11:1–284.